An Edge Detection Approach to Wideband Temporal Spectrum Sensing

Joseph M. Bruno, Brian L. Mark, Zhi Tian
Dept. of Electrical and Computer Engineering
George Mason University
email: { jbruno2, bmark, ztian1 }@gmu.edu

***Abstract*—In wideband spectrum sensing, an unlicensed user determines which portions of a given band have been left idle by the licensed users. A historical deficiency of wideband spectrum sensing, the inability to detect signals with low duty cycle, was addressed in a recent paper, where wideband temporal spectrum sensing was introduced. We propose an algorithm for reliable detection of low duty cycle signals in noisy environments. We leverage this recent advance in wideband spectrum sensing, and apply a well-known edge detection algorithm to determine channel boundaries. Numerical results are presented which show performance improvements over the original wideband temporal spectrum sensing algorithm, particularly in low signal-to-noise ratio scenarios.**[1]

***Index Terms*—Cognitive radio, spectrum sensing, hidden Markov model**

I. Introduction

Due to the rapidly increasing demand for capacity in wireless networks, radio frequency (RF) spectrum access is becoming more precious every day. However, it has been shown that fixed frequency allocations have left large portions of the RF spectrum underutilized [1]. Cognitive radio technologies aim to increase utilization of those bands without causing harmful disruption to the licensed or primary users (PUs) [2] by allowing unlicensed or secondary users (SUs) to opportunistically access such spectrum holes. In order to maximize capacity and minimize service disruptions to the PUs, a cognitive radio-enabled SU can employ sophisticated sensing techniques to characterize the spectrum holes within a given band.

The spectrum sensing task of an SU for a given band can classified as follows [3], [4]:

1) *Narrowband:* A single channel is clearly defined.
2) *Multiband:* A set of independent narrowband channels is given.
3) *Wideband:* The spectrum band is wide, and may contain multiple narrowband channels with unknown channel boundaries.

Of the three, narrowband sensing has been studied most extensively. Well-known detection algorithms for narrowband sensing include energy detection, cyclostationary feature detection, and matched filter detection [5]. Hidden Markov models (HMMs) and related models have been used to characterize the temporal behavior of the PU [6], [7]. In [8], multiband sensing is formulated as a problem of allocating spectrum sensing effort among a set of narrowband channels.

In the wideband spectrum sensing scenario, an SU must sense an entire band and determine channel boundaries. The bandwidth that must be sensed can vary from the order of 1 MHz to 1 GHz. This is required if the SU can not leverage any external information about channel allocation. A SU need only perform wideband sensing during initialization and may then revert to multiband or narrowband sensing during normal operation. In general, PU signals may be heterogeneous in frequency, bandwidth, and power, so robust wideband sensing algorithms must be developed to detect all PU activity within the spectrum band. Most state-of-the-art approaches for wideband sensing are based on wideband energy detection [9] or frequency-domain edge detection [10]. Edge detectors can offer an improvement over energy detectors in terms of signal-to-noise ratio (SNR) threshold, but they can also perform relatively poorly on signals with gradual rolloffs in their band edges. Neither technique takes into account the temporal dynamics of PU signals, and consequently both can perform rather poorly when PU signals have low duty cycles. Many advanced wideband spectrum sensing methods have been proposed which offer various improvements over standard wideband energy or edge detection but all model the PU state as either on or off, not changing over time [11]–[16].

In [4], a sensing framework for reliable wideband detection of PUs with low duty cycle was developed. The approach, referred to as wideband temporal sensing, involves partitioning the given spectrum band into smaller subchannels. The energy in each subchannel is measured and an HMM-based spectrum sensing approach is applied to each subchannel. A recursive tree search is performed to aggregate correlated subchannels into a set of independent narrowband channels, which effectively reduces the sensing task to the multiband case. The wideband temporal sensing approach developed in [4] allows PU signals with low duty cycle to be detected accurately at high to moderate SNR.

The main contribution of this paper is to apply an edge detection algorithm to wideband temporal sensing, which allows for more reliable detection at low SNR compared to the wideband temporal energy detector of [4]. Moreover, the use of edge detection avoids the need for the recursive tree search used in the wideband temporal energy detector,

[1]This work was supported in part by the U.S. National Science Foundation under Grants No. 1421869 and 1205453.

resulting in a computationally more efficient spectrum sensing scheme. Our approach incorporates the wavelet-based edge detection algorithm of [10] into the wideband temporal sensing framework proposed in [4]. We present experimental results obtained through simulation.

The remainder of the paper is organized as follows. In Section II, we define the system model for wideband spectrum sensing. In Section III, we discuss and evaluate the performance of two existing wideband spectrum sensing techniques. In Section IV, we develop the proposed edge detection approach to wideband temporal spectrum sensing. In Section V, we describe the simulation that was used to compare the proposed algorithm to existing algorithms and present numerical results. Concluding remarks are given in Section VI.

II. System Model

A. Wideband Channel Model

Over a given wideband spectrum band, we assume that an unknown number of independent PUs are operating. Each PU has an unknown center frequency and bandwidth. It is assumed that PU channels do not overlap in frequency. The channel over which a given PU is observed is assumed to be flat Rayleigh fading with parameter σ_f combined with additive white Gaussian noise (AWGN), defined by the circularly symmetric complex normal distribution $\mathcal{C}\left(0, \sigma_n^2\right)$. The mean SNR of the received signal on the PU channel, given that the PU is transmitting, is given by

$$\overline{\mathrm{SNR}} = \frac{\sigma_f^2}{\sigma_n^2}. \tag{1}$$

B. PU Traffic Model

A given PU may be transmitting or idle at any given time. The state of the PU is denoted by a discrete-time random process $X = \{X_k\}_{k=1}^{\infty}$, where $X_k = 1$ if the PU is idle or $X_k = 2$ if the PU is active at time k. We shall assume that the PU state process X is characterized by an ergodic time-homogeneous discrete-time Markov chain with transition matrix $G = [g_{ab} : a, b \in \{1, 2\}]$, where

$$g_{ab} = \mathrm{P}\left(X_2 = b \mid X_1 = a\right), \tag{2}$$

and initial distribution $\nu = [\nu_a : a = 1, 2]$, where

$$\nu_1 = \mathrm{P}\left(X_1 = 1\right),\ v_2 = \mathrm{P}\left(X_1 = 2\right). \tag{3}$$

The equilibrium state distribution, denoted by $\pi = [\pi_1, \pi_2]$, satisfies the following equations:

$$\pi = \pi G,\ \pi_1 + \pi_2 = 1. \tag{4}$$

The value π_2 corresponds to the duty cycle of the PU in steady-state.

C. Cognitive Receiver Model

1) Received Wideband Signal: In the active state, a transmitting PU will generate a bandpass signal $S = \{\tilde{S}_k\}_{k=1}^{\infty}$, where $\tilde{S}_k$ denotes the Inphase-Quadrature (IQ) sample at time k. The transmitted signal for the PU at time k is given by

$$S_k = \tilde{S}_k \cdot 1_{\{X_k = 2\}}, \tag{5}$$

where 1_A is the indicator function on the event A. The PU signal is multiplied at time k by a fading signal $f = f_k \sim \mathcal{C}\left(0, \sigma_f^2\right)$. All M PU signals are received simultaneously and added to the noise signal $N = \{N_k\}_{k=1}^{\infty}$, where $N_k \sim \mathcal{C}\left(0, \sigma_n^2\right)$. The received wideband signal is represented by $Z^{\mathrm{wb}} = \{Z_k^{\mathrm{wb}}\}$, where Z_k^{wb} is the k^{th} I-Q sample from the wideband channel.

2) Channelized Received Signal: The SU will partition the wideband received signal into J narrowband subchannels. Initially this division must be done arbitrarily, but after wideband sensing, the set of subchannels should describe all PU statistics as well as the statistics of the spectrum holes between PU signals. The signal corresponding to the j^{th} subband is denoted by $Z^{(j)}$.

3) Energy Detected Signal: For spectrum sensing, the channelized narrowband signals are processed with an averaging energy detector, which estimates the power of each sample and averages K samples together. The resulting received energy signal in subchannel j is denoted by $Y^{(j)} = \{Y_k^{(j)}\}$, where

$$Y_k^{(j)} = \frac{1}{K} \sum_{l=1}^{K} |Z_{(k-1)K+l}^{(j)}|^2. \tag{6}$$

A SU will need to detect slow changes in PU state to properly leverage spectrum holes, and because of this, we assume that the probability of a state change occurring during the energy estimation of a single sample to be minimal. Therefore, we assume that during an energy detection window the samples of $Y^{(j)}$ are independent, identically distributed. For relatively large K, $Y_k^{(j)}$ will approach a normal random variable due to the Central Limit Theorem.

If $Y^{(j)}$ represents the energy estimates of subchannel j of a PU characterized by state process X, the k^{th} sample from the received narrowband signal will be given by

$$Z_k^{(j)} \sim \begin{cases} \mathcal{C}\left(0, \sigma_n^2\right), & X_k = 1, \\ \mathcal{C}\left(0, \sigma_f^2 + \sigma_n^2\right), & X_k = 2. \end{cases} \tag{7}$$

The resulting energy estimates, $Y_k^{(j)}$, will be scaled chi-squared random variables with $2N$ degrees of freedom. We will denote a chi-squared distribution with D degrees of freedom by $\mathcal{X}^2\left(D\right)$. The output of the energy detector is given by

$$Y_k^{(j)} \sim \begin{cases} \frac{\sigma_n^2}{N}\mathcal{X}^2\left(2N\right), & X_k = 1, \\ \frac{\sigma_f^2 + \sigma_n^2}{N}\mathcal{X}^2\left(2N\right), & X_k = 2. \end{cases} \tag{8}$$

The mean and variance of a chi-squared distribution with D degrees of freedom are D and $2D$ respectively. Assuming that N is sufficiently large, $Y_k^{(j)}$ will be conditionally normal:

$$Y_k^{(j)} \sim \begin{cases} \mathcal{N}\left(2\sigma_n^2, \frac{4\sigma_n^4}{N}\right), & X_k = 1, \\ \mathcal{N}\left(2\sigma_f^2 + 2\sigma_n^2, \frac{4\left(\sigma_f^2 + \sigma_n^2\right)^2}{N}\right), & X_k = 2. \end{cases} \tag{9}$$

III. Comparison of Wideband Spectrum Sensing Techniques

It was shown in [4] that standard wideband detection methods are inadequate for PUs with low duty cycle. The edge detection algorithm from [10] was performed on a wideband signal with four orthogonal frequency division multiplexing (OFDM) carriers of varying duty cycle. It was demonstrated that as the duty cycle was reduced, the detector sensitivity was also reduced. Performance of the standard edge detector is shown in Fig. 1 for OFDM signals with SNR of 10 dB and varying duty cycles, where the shaded areas indicate detected spectrum holes. Clearly, the edge detector fails to correctly detect the two rightmost OFDM signals.

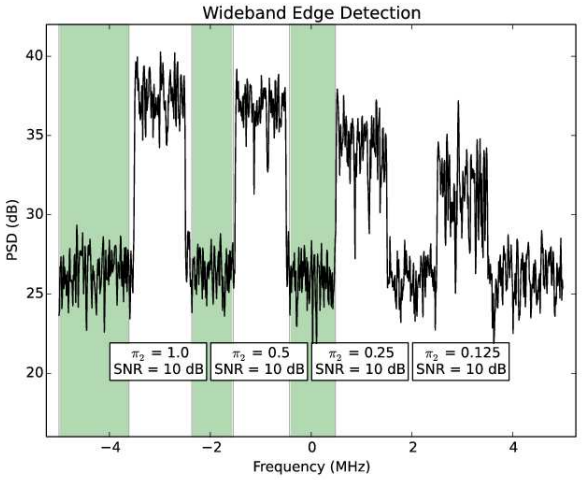

Fig. 1. Results of a wideband edge detector for OFDM signals with 10 dB SNR and 100%, 50%, 25%, and 12.5% duty cycles [4].

Wideband temporal spectrum sensing was introduced in [4] to more reliably detect a PU with low duty cycles, where the proposed algorithm performed comparably to energy detection for duty cycles of 1.0 and did not degrade substantially for lower duty cycles. Because we are extending the wideband temporal spectrum sensing algorithm from [4], we shall refer to the incumbent algorithm as *wideband temporal energy detection*. Performance of the wideband temporal energy detector is shown in Fig. 2 for OFDM signals with SNR of 10 dB and varying duty cycles.

Although wideband temporal energy detection has been shown to reliably detect PU signals at 10 dB SNR for a variety of duty cycles, spectrum sensing applications may demand accurate PU detection at substantially lower SNR. It can be seen in Fig. 3 that at higher noise levels, the wideband temporal energy detection algorithm proposed in [4] begins to experience detection errors. Note that the wideband temporal energy detector incorrectly characterizes the rightmost spectrum hole. The edge detection algorithm proposed in [10] allows for accurate detection of high duty cycle signals in high noise levels, which motivates the development of an algorithm that extends wideband temporal spectrum sensing with edge detection.

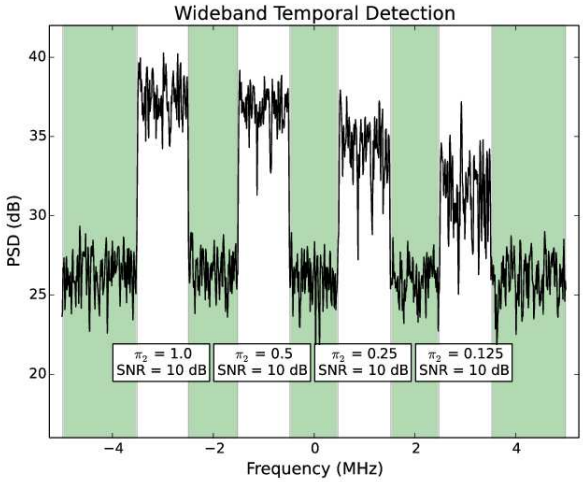

Fig. 2. Results of a wideband temporal energy detector for OFDM signals with 10 dB SNR and 100%, 50%, 25%, and 12.5% duty cycles [4].

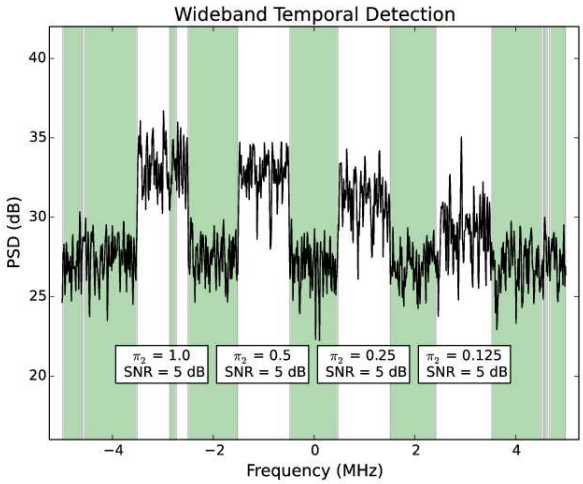

Fig. 3. Results of wideband temporal energy detector for OFDM signals with 5 dB SNR and 100%, 50%, 25%, and 12.5% duty cycles [4].

IV. Proposed Algorithm

In this section, we extend the wideband temporal sensing algorithm from [4]. Since the proposed algorithm uses edge

detection to determine channel boundaries, the recursive tree search used in [4] for channel aggregation is not necessary.

A. Channelization of Received Wideband Signal

First, the received wideband signal is divided into J narrowband signals of equal bandwidth. The narrowband signals are spaced such that they are non-overlapping and cover the entire band. Selection of J depends on the desired sensing resolution, W_r. Signals narrower than W_r may not be reliably detected, and detected channel boundary locations may have a frequency error as large as $\frac{W_r}{2}$. The number of subchannels required to achieve sensing resolution W_r is given by

$$J = \left\lceil \frac{W_0}{W_r} \right\rceil, \tag{10}$$

where W_0 is the width of the entire band. Channelization may be accomplished in a conceptually simple fashion using a bank of digital downconverters or more efficiently using a frequency-domain channelizer, as described in [4, Sec. III-b]. If a frequency-domain channelizer is used, J from Eq. (10) should be rounded up to the next power of 2 for efficient FFT computation. The resulting set of all J narrowband received signals is denoted by $\boldsymbol{Z} = \left\{Z^{(1)}, \ldots, Z^{(J)}\right\}$.

B. Sensing of Narrowband Subchannels

The observation of PU traffic through a noisy channel can be accurately modelled using a hidden Markov model (HMM), denoted by (Y, X), where X is an underlying discrete-time Markov chain and Y is a random sequence of observations, conditionally dependent on X. The transition matrix and initial distribution of the HMM are given in (2) and (3), respectively. The noisy samples are modeled by normal distributions. The parameter of the HMM for a PU is given by $\phi = (\nu, G, \mu, \Sigma)$, where $\mu = [\mu_1, \mu_2]$ and $\Sigma = \left[\sigma_1^2, \sigma_2^2\right]$ are, respectively, the sets of conditional means and conditional variances for subchannel j given by (9).

For a set of J subchannels that partition a spectrum band evenly, the conditional means

$$\boldsymbol{\mu}_a = \left\{\mu_a^{(1)}, \ldots, \mu_a^{(J)}\right\}, \ a = 1, 2, \tag{11}$$

determine the *conditional power spectral density* of the received signals on the subchannels. If the J uniformly distributed channels which cover the band have frequencies $\{f_1, \ldots, f_J\}$, the conditional power spectral densities are defined as

$$\mu_a(f) = \sum_{j=1}^{J} \frac{\mu_a^{(j)}}{\Delta_f} \mathrm{rect}\left(\frac{f - f_j}{\Delta_f}\right), \ a = 1, 2, \tag{12}$$

where $\mathrm{rect}(\cdot)$ denotes the unit rectangular function and Δ_f is the frequency spacing between subchannels. Here, $\mu_1(f)$ is the power spectral density of the received signal given that all PUs are idle, and $\mu_2(f)$ is the power spectral density of the received signal given that all PUs are transmitting.

For each of the J narrowband subchannels, energy detection and HMM parameter estimation is performed. The set of observed energy sequences is denoted $\boldsymbol{Y} = \left\{Y^{(1)}, \ldots, Y^{(J)}\right\}$ and is given by Eq. (6). Subchannel j is characterized by an HMM parameter, $\phi^{(j)} = \left(\nu^{(j)}, G^{(j)}, \mu^{(j)}, \Sigma^{(j)}\right)$, which is estimated using the Baum-Welch algorithm [17]. In the wideband temporal energy detector proposed in [4], the set of HMM parameters for the entire band is used directly.

Our performance baseline will be the wideband temporal energy detector from [4], which directly computes $\mu_2(f)$ from the conditional power spectral density, defined in Eq. (12), with a threshold λ to determine which subchannels contain an active PU. The adjacent active subchannels which are determined to be correlated are combined into a single channel.

C. Edge Detection

In our proposed algorithm, we apply the wideband edge detection algorithm from [10] to the conditional power spectral density of the received signal. We first decompose the conditional power spectral density into a set of resolutions using the continuous wavelet transform (CWT). The CWT of $\mu_2(f)$ for a resolution γ is given as

$$\mathcal{W}_\gamma \left\{\mu_2(f)\right\} = \mu_2(f) * \psi_\gamma(f), \tag{13}$$

where $*$ denotes convolution and $\psi_\gamma(f)$ is a wavelet of scale γ, given by

$$\psi_\gamma(f) = \frac{1}{\gamma} \psi\left(\frac{f}{\gamma}\right). \tag{14}$$

The mother wavelet, $\psi(t)$, is the Ricker wavelet, defined in [18, Eq. (4.34)] as

$$\psi(t) = \frac{2}{\pi^{1/4}\sqrt{3\sigma}} \left(\frac{t^2}{\sigma^2} - 1\right) \exp\left(\frac{-t^2}{2\sigma^2}\right). \tag{15}$$

The Ricker wavelet is the second derivative of a Gaussian function, and a standard Ricker wavelet, where $\sigma = 1$, is particularly useful for edge detection [18]. The r^{th} resolution of the conditional power spectral density has scale γ where $\gamma = 2^r$ and $r \in \{1, 2, \ldots, R\}$, where R is the number of CWT resolutions.

Once the conditional power spectral density is decomposed into component resolutions using the CWT, edge detection is performed by taking the first derivative of each component resolution:

$$\mathcal{W}'_\gamma \left\{\mu_2(f)\right\} = \gamma \frac{d}{df} \left(\mu_2(f) * \psi_\gamma(f)\right). \tag{16}$$

We then compute the multiscale wavelet product from the resulting gradient estimates:

$$\mathcal{U}_R \left\{\mu_2(f)\right\} = \prod_{r=1}^{R} \mathcal{W}'_\gamma \left\{\mu_2(f)\right\} \Big|_{\gamma = 2^r}. \tag{17}$$

By multiplying the component resolutions together, the signal is amplified, while the noise is not, resulting in noise suppression [19]. The resulting peaks in $\mathcal{U}_R \left\{\mu_2(f)\right\}$ are determined to be channel boundaries.

V. Simulation and Results

A. Simulation Setup

We tested the proposed wideband temporal edge detector against the wideband temporal energy detector from [4]. Wideband signals with OFDM carriers were tested. A duty cycle of $\pi_2 = 0.1$ was used, and SNR values of 0, 5, and 10 dB were tested. A total bandwidth of 10 MHz with four randomly placed PU signals was tested. The bandwidth and center frequency of each non-overlapping PU carrier were randomly generated each iteration, and the PU signal bandwidths were drawn randomly within the range 0.5 to 2.0 MHz. The full set of simulation parameters is enumerated in Table I. Note that the number of CWT resolutions (R) applies only to the edge detector.

Simulation Parameter	Value
Modulation	OFDM
Total bandwidth (W)	10 MHz
Duty cycle (π_2)	0.1
SNR	$\{0, 5, 10\}$ dB
Number of PU carriers	4
Number of narrowband subchannels (J)	1024
Energy detector average length (N)	10
Number of CWT resolutions (R)	4
Sensing duration per iteration	0.01 s
Number of simulation iterations	10000

TABLE I
Simulation parameters.

B. Qualitative Results

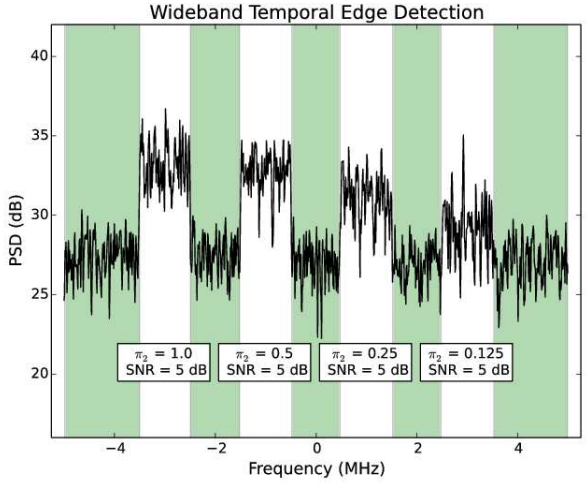

Fig. 4. Results of the proposed wideband temporal edge detector for OFDM signals with 10 dB SNR and 100%, 50%, 25%, and 12.5% duty cycles [4].

The visual output of the proposed wideband temporal edge detector is shown in Fig. 4, where the proposed detector was tested against a wideband signal with PUs of varying duty cycle with 5 dB SNR. This performance may be contrasted with the wideband temporal energy detector proposed in [4] in 5 dB SNR plotted in Fig. 3. Visually, it can be seen that the proposed wideband temporal edge detector performs accurately in relatively low SNR.

C. Numerical Results

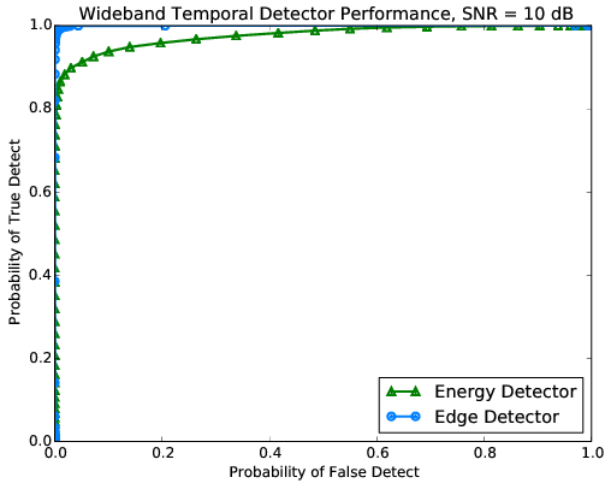

Fig. 5. Results of wideband temporal detectors for OFDM signals with 10 dB SNR.

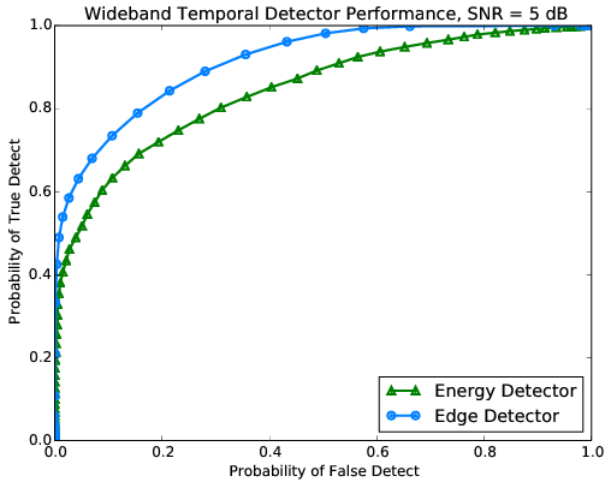

Fig. 6. Results of wideband temporal detectors for OFDM signals with 5 dB SNR.

Next, we present numerical results demonstrating the performance improvement achieved by wideband temporal edge detection for a variety of medium to low SNR signals. In each simulation iteration, every narrowband channel was recorded as either a true detect, a true positive, a false detect, or a false positive, depending on the known PU signal locations and the detector results. A variety of thresholds were tested so that the relationship between detection rates can be observed. Averaged detection characteristics are plotted as receiver operating characteristic (ROC) curves. The resulting plots are shown in Fig. 5, 6, and 7 for SNRs of 10, 5, and 0 dB, respectively. From these results, it is apparent that the wideband temporal edge detector performs favorably compared to the wideband

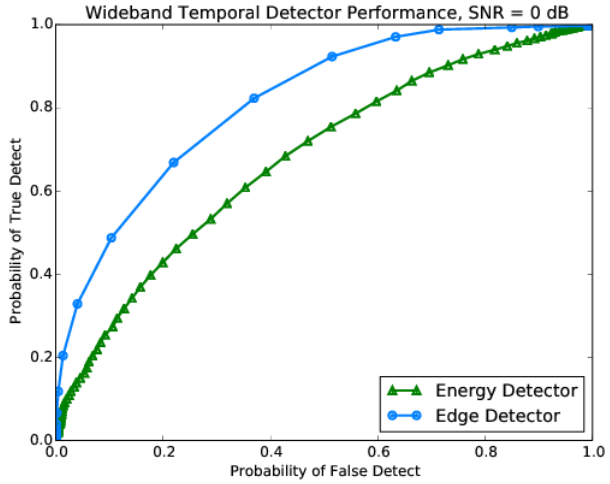

Fig. 7. Results of wideband temporal detectors for OFDM signals with 0 dB SNR.

temporal energy detector from [4] for all simulated SNR values. The performance benefit of edge detection is especially pronounced at the low SNR of 0 dB. The simulated duty cycle of $\pi_2 = 0.1$ was lower than any duty cycle simulated in [4], and the wideband temporal energy detector produced similar results to those in [4] at 10 dB SNR.

VI. Conclusion

We have proposed a wideband spectrum sensing algorithm that is capable of detecting PU signals at low duty cycles and relatively low SNR. We leveraged the wideband temporal sensing framework introduced in [4], which had been shown to perform well for low duty cycle PU signals at moderate SNR. We enhanced the wideband temporal sensing framework with the edge detection algorithm from [10]. This enhancement was shown to perform substantially better at lower SNR, making the proposed algorithm more suitable for cognitive radio tasks that require highly reliable detection at low to moderate SNR.

Several extensions to the proposed algorithm are being investigated in our ongoing work. One such extension is failure detection, where the SU would detect that no signal edges are present and default to wideband temporal energy detection, which would allow for sensing of PU signals without sharp band edges, as discussed in [4]. Another extension to the proposed sensing algorithm involves smoothing of the conditional power spectral density in Eq. (12) using the maximum a posteriori (MAP) decisions produced by the Baum-Welch algorithm to more reliably estimate average received signal power.

References

[1] Federal Communications Commission (FCC), "Spectrum policy task force," Rep. ET Docket, Federal Communications Commission, Tech. Rep. 02-135, Nov. 2002.

[2] S. Haykin, "Cognitive radio: Brain-empowered wireless communications," *IEEE J. Sel. Areas Commun.*, vol. 23, no. 2, pp. 201–220, Sep. 2006.

[3] H. Sun, A. Nallanathan, C.-X. Wang, and Y. Chen, "Wideband spectrum sensing for cognitive radio networks: a survey," *IEEE Wireless Commun. Mag.*, vol. 20, no. 2, pp. 74–81, April 2013.

[4] J. M. Bruno and B. L. Mark, "A recursive algorithm for joint time-frequency wideband spectrum sensing," in *Proc. IEEE Int. Workshop on Smart Spectrum (IWSS), Wireless Communications and Networking Conference Workshops (WCNCW)*, March 2015, pp. 235–240.

[5] T. Yucek and H. Arslan, "A survey of spectrum sensing algorithms for cognitive radio applications," *IEEE Commun. Surveys Tuts.*, vol. 11, no. 1, pp. 116–130, March. 2009.

[6] I. Akbar and W. Tranter, "Dynamic spectrum allocation in cognitive radio using hidden markov models: Poisson distributed case," in *Proc. IEEE SoutheastCon 2007*, March 2007, pp. 196–201.

[7] T. Nguyen, B. L. Mark, and Y. Ephraim, "Spectrum sensing using a hidden bivariate Markov model," *IEEE Trans. Wireless Commun.*, vol. 12, no. 9, pp. 4582–4591, Aug. 2013.

[8] P. Tehrani, L. Tong, and Q. Zhao, "Asymptotically efficient multi-channel estimation for opportunistic spectrum access," *IEEE Trans. Signal Process.*, vol. 60, no. 10, pp. 5347–5360, Oct. 2012.

[9] D. Cabric, S. Mishra, and R. Brodersen, "Implementation issues in spectrum sensing for cognitive radios," in *Proc. Thirty-Eighth Asilomar Conference on Signals, Systems and Computers*, vol. 1, Nov. 2004, pp. 772–776.

[10] Z. Tian and G. B. Giannakis, "A wavelet approach to wideband spectrum sensing for cognitive radios," in *Proc. 1st Int. Conf. on Cog. Radio Oriented Wireless Nets. and Comms. (CROWNCOM)*, June 2006, pp. 1–5.

[11] A. Mariani, A. Giorgetti, and M. Chiani, "Wideband spectrum sensing by model order selection," *IEEE Transactions on Wireless Communications*, vol. 14, no. 12, pp. 6710–6721, Dec 2015.

[12] R. Lopez-Valcarce and G. Vazquez-Vilar, "Wideband spectrum sensing in cognitive radio: Joint estimation of noise variance and multiple signal levels," in *Proc. IEEE 10th Workshop on Signal Processing Advances in Wireless Communications*, June 2009, pp. 96–100.

[13] M. Sanna and M. Murroni, "Opportunistic wideband spectrum sensing for cognitive radios with genetic optimization," in *Proc. IEEE Int. Conf. on Communications (ICC)*, May 2010, pp. 1–5.

[14] T. H. Yu, S. Rodriguez-Parera, D. Markovic, and D. Cabric, "Cognitive radio wideband spectrum sensing using multitap windowing and power detection with threshold adaptation," in *Proc. IEEE Int. Conf. on Communications (ICC)*, May 2010, pp. 1–6.

[15] D. Bao, L. D. Vito, and S. Rapuano, "A histogram-based segmentation method for wideband spectrum sensing in cognitive radios," *IEEE Trans. on Instrumentation and Measurement*, vol. 62, no. 7, pp. 1900–1908, July 2013.

[16] L. Angrisani, G. Betta, D. Capriglione, G. Cerro, L. Ferrigno, and G. Miele, "Proposal and analysis of new algorithms for wideband spectrum sensing in cognitive radio," in *Proc. IEEE Int. Instrumentation and Measurement Technology Conf. (I2MTC)*, May 2014, pp. 701–706.

[17] L. E. Baum and T. Petrie, "Statistical inference for probabilistic functions of finite state Markov chains," *Annals of Mathematical Statistics*, vol. 37, no. 6, pp. 1554–1563, Apr. 1966.

[18] S. Mallat, *A wavelet tour of signal processing: the sparse way*, 3rd ed. Academic Press, 2009.

[19] B. M. Sadler and A. Swami, "Analysis of multiscale products for step detection and estimation," *IEEE Trans. Inf. Theory*, vol. 45, no. 3, pp. 1043–1051, 1999.